Statistical theory of energy loss and charge exchange of penetrating particles: Energy-loss spectra and applications

Andreas Närmann*
Fysisk Institut, Odense Universitet, DK-5230 Odense M, Denmark
(Received 6 July 1994)

A recently presented formalism for the computation of energy-loss spectra of penetrating particles in the presence of charge exchange has been extended to include analytical expressions for energy-loss spectra in the diffusion approximation. For a two-state system the case of charge transfer in one direction only, as well as in both directions, is investigated. Expressions obtained for charge-state distributions are evaluated, using theoretically and experimentally determined cross sections.

PACS number(s): 34.50.Bw, 34.70.+e, 52.40.Hf, 61.80.Mk

I. INTRODUCTION

A theory describing the energy loss of charged particles in the presence of charge exchange was recently presented [1,2]. General expressions were derived for the mean energy loss and straggling in equilibrium. This work was extended in [3] to include higher moments of the energy-loss distribution and transients. Concerning the historical development of this area of research, the reader is referred to Ref. [2], which also includes an extensive list of references.

Up to now formulas were derived in [1–3] for important experimental parameters such as the charge-state distribution and the energy-loss spectrum integrated over all exit charge states. Mean energy loss, straggling, and skewness were given analytically and separated into an equilibrium and a transient part, the latter one depending on the initial charge state. Charge-state distributions have not been evaluated for real systems and analytical expressions for energy-loss spectra resolved for the exit charge have not been extracted yet.

The advantage of this formalism is that it delivers expressions for the experimentally relevant quantities in a closed, algebraic form, so that one does not have to resort to Monte Carlo methods.

This paper concentrates on applying the equations obtained for charge-state distributions to real systems and on deriving formulas for energy-loss spectra for the two-state case in the diffusion approximation. It will be shown that expressions derived earlier for a special case (He^+ particles incident on Ni surfaces) [4] are also contained in this description.

II. INPUT AND OUTPUT

In this section the results of [1,2] are briefly summarized and the main quantities used in this paper are introduced.

The key input is a set of differential transition rates $d\Lambda_{IJ}(T)/dT$ between accessible projectile states I and J, defined such that $[d\Lambda_{IJ}(T)/dT]dT\delta t \equiv \delta t d\Lambda_{IJ}(T)$ is the probability in a small time interval δt for a transition from state I to state J under simultaneous loss of kinetic energy (T, dT). In standard penetration theory [1], only collisional interactions are considered so that transition rates reduce to $d\Lambda_{IJ}(T) = Nvd\sigma_{IJ}(T)$, where N is the density of scattering centers, v the projectile velocity, and $d\sigma_{IJ}(T)$ the differential cross section. The notation in terms of transition rates allows for both spontaneous and collisionally induced events [2].

The most general output is a transfer matrix $\mathbf{F}(\Delta E, t) = \{F_{IJ}(\Delta E, t)\}$. Here $F_{IJ}(\Delta E, t)d(\Delta E)$ is the probability for a projectile occupying state I at $t = 0$ to occupy state J at time t and to have lost kinetic energy $(\Delta E, d(\Delta E))$ by an arbitrary sequence of events. $\mathbf{F}(\Delta E, t)$ has been found to obey a generalized Bothe-Landau formula [1]

$$\mathbf{F}(\Delta E, t) = \frac{1}{2\pi}\int_{-\infty}^{\infty} dk e^{ik\Delta E}\, e^{t[\mathbf{Q}-\mathbf{\Lambda}(k)]}, \tag{1}$$

where $Q_{IJ} = \int d\Lambda_{IJ} - \delta_{IJ}\sum_L \int d\Lambda_{IL}$ and $\Lambda_{IJ}(k) = \int d\Lambda_{IJ}(1 - e^{-ikT})$. Equation (1) assumes the individual events to be statistically independent and transition rates $d\Lambda_{IJ}(T)/dT$ to be independent of time.

The charge-state distribution $F_{IJ}(t)$ at time t is obtained from Eq. (1) by integration over ΔE,

$$\mathbf{F}(t) = e^{t\mathbf{Q}}. \tag{2}$$

The matrix $\mathbf{Q}$ satisfies the important sum rule $\sum_J Q_{IJ} = 0$.

In this paper Eq. (1) will be evaluated for some special cases. For very simple systems analytical expressions are available but for more complex ones numerical methods were applied. The time variable t will be changed to the experimentally more relevant thickness $x = vt$, where v is the projectile's incident velocity which is assumed to be constant.

*Present address: Universität Osnabrück, Fachbereich Physik, D-49069 Osnabrück, Federal Republic of Germany.

III. CHARGE-STATE STATISTICS

Methods to evaluate the charge-state distribution [Eq. (2)] have been outlined in [5].

Arnau *et al.* [6] calculated the transition rates of electron capture and loss for a proton in aluminum in density functional formalism as a function of the projectile's velocity. The accessible states are H^+ (state 1), H^0 (2), and H^- (3). These transition rates are input to Eq. (2) and yield, e.g., the function F_{12} displayed in Fig. 1. It is only for the medium range of velocities (about 1 Bohr velocity) that there is a significant amount of neutrals emerging at larger thicknesses. At low velocity the production of H^- is very efficient, thus emptying the H^0 state, and at high velocities the H^+ state is preferred, thus inhibiting further population of H^0.

As a second example, recently published results [7] about charge-state distributions of fast oxygen ions exiting carbon foils are applied. Wagner *et al.* determined equilibrium and nonequilibrium distributions and extracted the charge-changing cross sections. Figure 2 shows the charge-state fraction obtained from their numbers and the experimental data. The excellent agreement is not too surprising since the cross section data input into Eq. (2) are derived from the same experiment to which we compare the resulting curves. However, the above procedure shows that the obtained results are consistent.

The advantage of this method is computational speed. Especially when many states are involved, evaluating a matrix exponential numerically is faster than solving a set of differential equations. This task is facilitated appreciably by using computer algebra programs.

This method can also be used in the case of incomplete sets of cross sections. By guessing the missing cross sections and comparing to the experimentally obtained charge-state distribution, one obtains estimates for those cross sections. This does not necessarily produce unique cross sections, though.

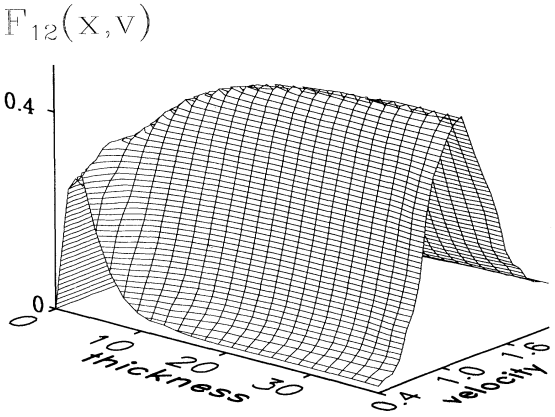

FIG. 1. Element F_{12} of the transfer matrix. State 1 corresponds to H^+, state 2 to H^0, for further details see text. Projectile velocity is given in units of v_B, the Bohr velocity, thickness in units of a_0, the Bohr radius, and the transfer matrix element in units of inverse hartrees (1 hartree = 27.2 eV.)

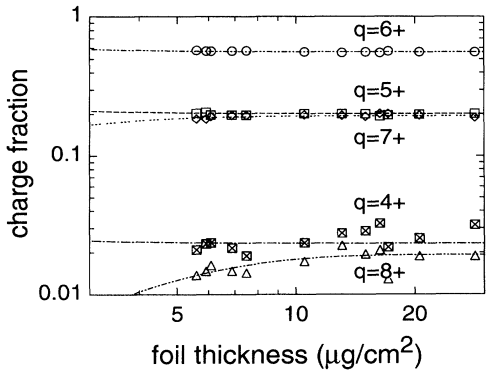

FIG. 2. Calculated charge fraction for 13 MeV $O^{3+} \rightarrow$ C foil. The lines are obtained from evaluating Eq. (2); markers are experimental data by Wagner *et al.*.

IV. ENERGY-LOSS SPECTRA FOR THE TWO-STATE CASE IN THE DIFFUSION APPROXIMATION

The aim of this section is to extract energy-loss spectra from Eq. (1) instead of averaged quantities. For the important case of two accessible states analytical expressions can be derived in the diffusion approximation.

For thick targets, i.e., large x, the diffusion approximation can be applied: the exponential in $\Lambda_{IJ}(k) = \int d\Lambda_{IJ}\left(1 - e^{-ikT}\right)$ is expanded up to the third term and yields

$$\mathbf{\Lambda}(k) \simeq ik\mathbf{S} + k^2\mathbf{W}/2, \tag{3}$$

where $S_{IJ} = \int d\Lambda_{IJ} T$ is the stopping cross section and $W_{IJ} = \int d\Lambda_{IJ} T^2$ the straggling parameter.

In the following, off-diagonal elements in stopping and straggling are ignored [8], i.e., energy loss and straggling due to charge exchange events are not taken into account. For simplicity the notation $S_{II} = S_I$ and $W_{II} = W_I$ is introduced.

The exponential matrix in Eq. (1) can be evaluated analytically for the two-state case. In the next steps further simplifying approximations to the resulting expressions for the elements of the transfer matrix will be applied.

A. One-way charge exchange only

If charge exchange is allowed to occur in one direction only, i. e., $\sigma_{12} \neq 0$ and $\sigma_{21} = 0$, one obtains for F_{11}

$$\begin{aligned} F_{11}(\Delta E, x) &= \frac{1}{2\pi}\int dk\; e^{ik(\Delta E - S_1 N x)} e^{-k^2 W_1 N x/2 - \sigma_{12} N x} \\ &= \frac{1}{\sqrt{2\pi W_1 N x}} e^{-\sigma_{12} N x} \\ &\quad \times \exp\left(-\frac{(\Delta E - S_1 N x)^2}{2 W_1 N x}\right), \end{aligned} \tag{4}$$

which is the expected Gaussian distribution.

The energy-loss distribution at penetrated thickness x of all particles with state 1 as initial and state 2 as final state is given by the expression

$$F_{12}(\Delta E,x) = f_2(\Delta E,x) - e^{-\sigma_{12}Nx} f_1(\Delta E,x), \qquad (5)$$

where

$$f_I(\Delta E,x) = \frac{\sigma_{12}}{2\pi}\int dk\; e^{ik(\Delta E - S_I Nx)} \times \frac{\exp(-k^2 W_I Nx/2)}{\sigma_{12} + k^2\Delta W/2 + ik\Delta S}, \qquad (6)$$

with $\Delta S = S_1 - S_2$ and $\Delta W = W_1 - W_2$.

1. Negligible difference in straggling

If $W_1 = W_2 \equiv W$ in Eq. (6), the integrals can be expressed in terms of the error function:

$$f_I(\Delta E,x) = c\exp\left(-\frac{\sigma_{12}}{\Delta S}(\Delta E - S_I Nx)\right) \times\left[1 + \mathrm{erf}\left(\frac{\Delta E - S_I Nx}{\sqrt{2WNx}} - \frac{\sigma_{12}}{\Delta S}\sqrt{WNx/2}\right)\right], \qquad (7)$$

$$c = \frac{\sigma_{12}}{2\Delta S}\exp\left[\frac{1}{2}\left(\frac{\sigma_{12}}{\Delta S}\right)^2 WNx\right].$$

In the equilibrium limit (large x), the second term in Eq. (5) vanishes. Then we arrive at the same expression which was already derived in [4] using a different approach.

2. Different straggling in both states

If straggling in the two states is different, the final expression can still be written in the form of Eq. (5) with the functions f_I now being

$$f_I(\Delta E,x) = c[e^{W_I Nxk_2^2/2} G_{I,k_2}(\Delta E,x) - e^{W_I Nxk_1^2/2} G_{I,k_1}(\Delta E,x)], \qquad (8)$$

$$G_{I,k}(\Delta E,x) = e^{(\Delta E - S_I Nx)k}\mathrm{erf}\left(\frac{\Delta E - S_I Nx}{2\sqrt{W_I Nx/2}} + k\sqrt{W_I Nx/2}\right)(\sigma_{12}/k - \Delta Wk/2 - \Delta S) + e^{-(\Delta E - S_I Nx)k}\mathrm{erf}\left(-\frac{\Delta E - S_I Nx}{2\sqrt{W_I Nx/2}} + k\sqrt{W_I Nx/2}\right)(\sigma_{12}/k - \Delta Wk/2 + \Delta S), \qquad (9)$$

$$c = \frac{\sigma_{12}}{\Delta W^2(k_1^2 - k_2^2)}\exp\left[\frac{1}{2}\left(\frac{\sigma_{12}}{\Delta S}\right)^2 WNx\right], \qquad (10)$$

where the k_i are given by the following relation:

$$k_{1,2}^2 = 2\left[\frac{\sigma_{12}}{\Delta W} + \left(\frac{\Delta S}{\Delta W}\right)^2\right] \pm 2\frac{\Delta S}{\Delta W}\sqrt{\left(\frac{\Delta S}{\Delta W}\right)^2 + 2\frac{\sigma_{12}}{\Delta W}}. \qquad (11)$$

B. Charge exchange in both directions

Now charge exchange in both directions is allowed for, i.e., both transition rates are larger than zero. Again, straggling in the two states is set to be the same.

The elements of the transfer matrix can be shown to give

$$F_{11}(\Delta E,x) = A\int_0^\infty dt\;[\sinh t\cos(\alpha\beta\cosh t)\cos(\tfrac{1}{2}\beta\sinh t) + \cosh t\sin(\alpha\beta\cosh t)\sin(\tfrac{1}{2}\beta\sinh t)\,] \times\exp(-\varepsilon\beta^2\cosh^2 t) + A\int_0^{\pi/2} dt\;[\cos t\cos(\alpha\beta\sin t)\cosh(\tfrac{1}{2}\beta\cos t) + \sin t\sin(\alpha\beta\sin t)\sinh(\tfrac{1}{2}\beta\cos t)\,] \times\exp(-\varepsilon\beta^2\sin^2 t) \qquad (12)$$

and

$$F_{12}(\Delta E,x) = 2A'\int_0^\infty dt\cos(\alpha\beta\cosh t)\sin(\tfrac{1}{2}\beta\sinh t) \times \exp(-\varepsilon\beta^2\cosh^2 t) + 2A'\int_0^{\pi/2} dt\cos(\alpha\beta\sin t)\ \sinh(\tfrac{1}{2}\beta\cos t) \times \exp(-\varepsilon\beta^2\sin^2 t)\ . \quad (13)$$

Here the following abbreviations are introduced:

$$\alpha = \frac{1}{\Delta S N x}\left(\Delta E - \overline{S}Nx - \frac{W}{\Delta S}\Delta\sigma Nx\right),$$
$$\beta = 2\sqrt{\sigma_{12}\sigma_{21}}Nx,$$
$$\varepsilon = \frac{WNx}{2(\Delta S N x)^2},$$

and the coefficients are given by

$$A = \frac{\beta}{\pi|\Delta S N x|}e^{-\overline{\sigma}Nx}\exp\left(-\frac{\Delta\sigma}{\Delta S}(\Delta E - \overline{S}Nx) + \frac{\Delta\sigma}{\Delta S}^2\frac{1}{2}WNx\right)$$
$$A' = \frac{\sigma_{12}Nx}{\beta}A\ ,$$

with $\Delta S = S_1 - S_2$, $\Delta\sigma = \sigma_{12} - \sigma_{21}$, $\overline{S}$ mean stopping, $\overline{\sigma}$ mean transition rate, ΔE the energy-loss variable, W the straggling parameter, and Nx the thickness variable.

F_{22} can be obtained from Eq. (12) by substituting the two plus signs under the integrals by minus signs and $F_{21}(\Delta E,x) = (\sigma_{21}/\sigma_{12})F_{12}(\Delta E,x)$.

In the following evaluation the same set of parameters as in [4] is used, i.e., corresponding to the interaction of a 5 keV He particle with a free electron gas. The He^+ ion is chosen as the incident state (1), which is subject to neutralization (to He^0, state 2) and reionization according to the transition rates $Nv\sigma_{12}$ and $Nv\sigma_{21}$. Numbers

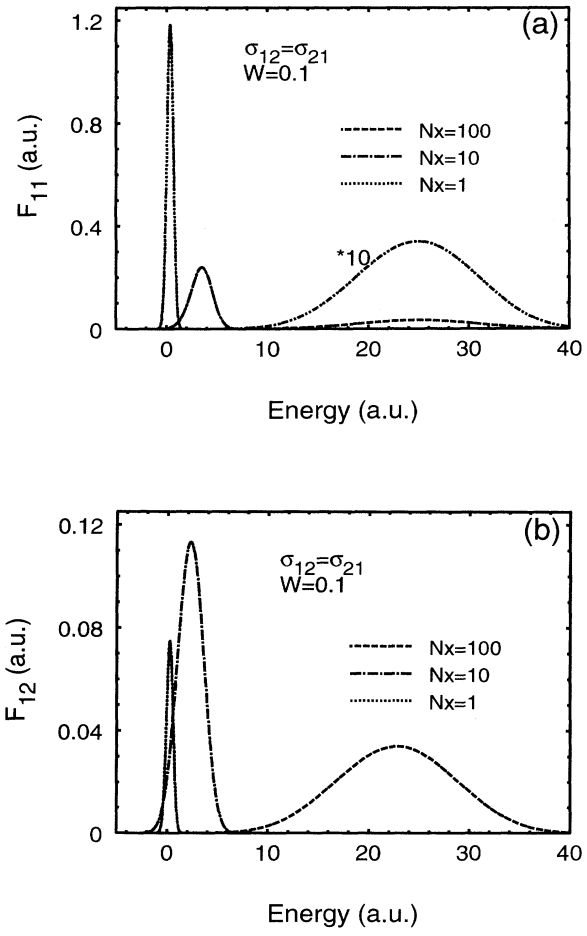

FIG. 3. Transfer matrix elements F_{11} (a) and F_{12} (b) for the case of equal transition probabilities and different thicknesses.

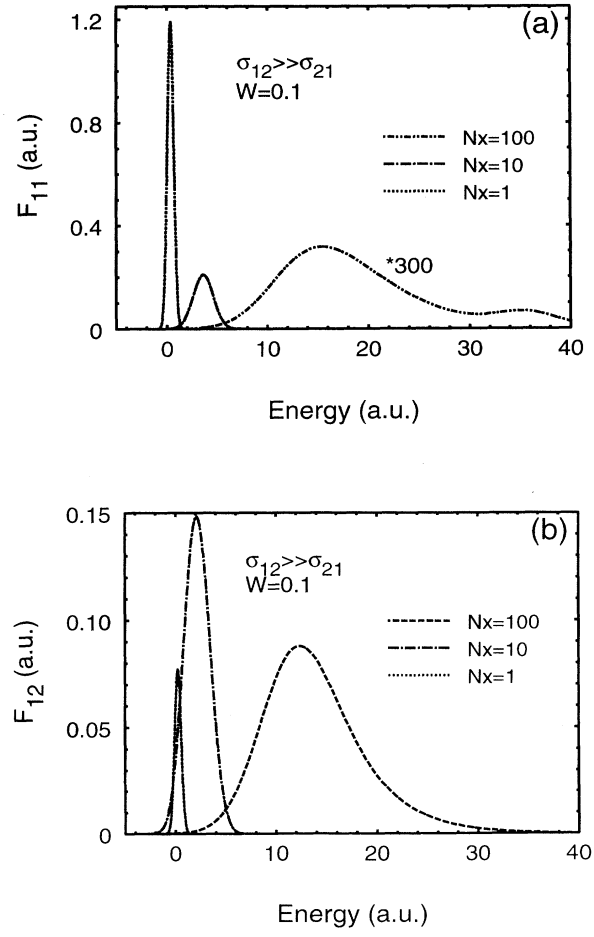

FIG. 4. Transfer matrix elements F_{11} (a) and F_{12} (b) for the case of one transition probability being much larger than the second one, each shown for different thicknesses.

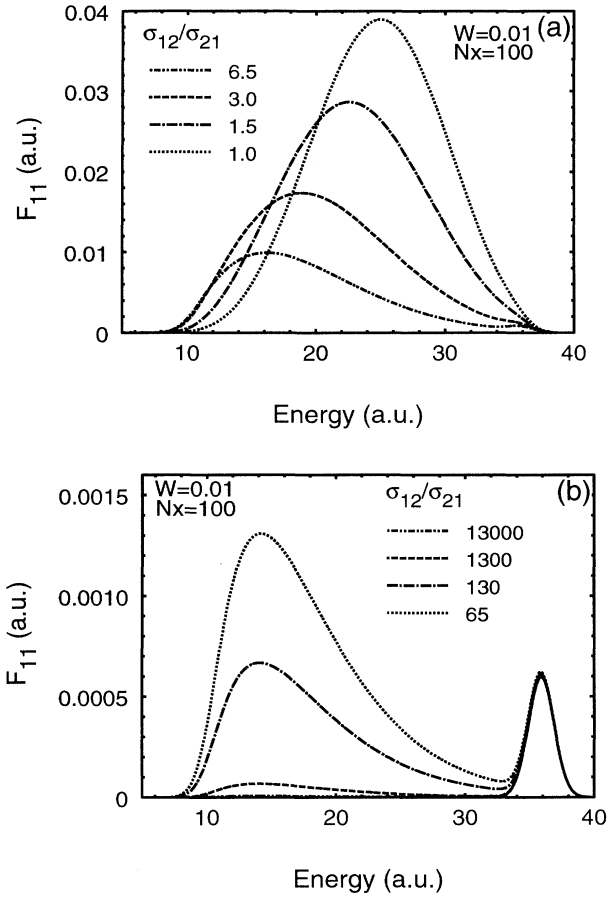

FIG. 5. Transfer matrix element F_{11} for two different ranges of ratios σ_{12}/σ_{21}, where σ_{12} was kept fixed at 0.065 a.u.

given are always in atomic units unless stated otherwise: $\sigma_{12} = 0.065$, $S_2 = 0.097$, and $S_1 = 3.7 \times S_2$.

Figure 3 shows the evolution of the transfer matrix elements with increasing thickness for the case that $\sigma_{21} = \sigma_{12}$. Figure 4 displays the same series for $\sigma_{21} \ll \sigma_{12}$. Here one sees that for large thickness a new feature appears in the spectrum. In order to further investigate this structure, straggling was reduced by a factor of 10 and the transfer matrix element was calculated for large thickness for different ratios σ_{12}/σ_{21}, where σ_{12} was kept constant. The resulting curves are shown in Fig. 5.

Finally, Fig. 6 shows all four matrix elements for a fixed ratio σ_{12}/σ_{21} and the same set of other parameters.

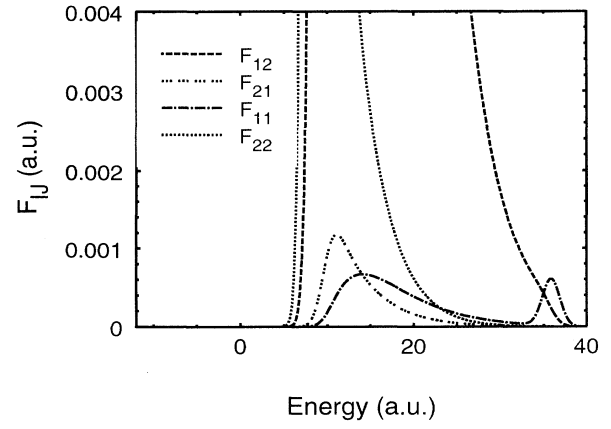

FIG. 6. Transfer matrix elements F_{IJ} for $\sigma_{12}/\sigma_{21} = 130$; all other parameters as in Fig. 5.

V. DISCUSSION

In the limit of large x Eqs. (5) and (7) yield the same expression that was already derived in [4] [Eq. (8)]. That paper deals with specular surface scattering of He^+ particles under grazing incidence off a Ni(110) surface along a random (high indexed) azimuthal direction. This geometry makes sure that only particles are detected which did not penetrate the uppermost atomic layer and thus only interacted with the electron density above the surface. Since the transition rates for neutralization and reionization of the incident particle depend on the electron density, the transition rates vary with time during the passage of the particle through the region of interaction. In Ref. [4] an average transition rate was used and in this approximation the same energy-loss formula was derived. In Sec. II the assumption was made that the transition rates $d\Lambda_{IJ}(T)/dT$ are independent of time. If the rates vary in a controlled way, the substitution $td\Lambda_{IJ}(T) \to \int_0^t dt' d\Lambda_{IJ}(t', T)$ may be utilized.

Now the energy-loss spectra obtained from Eqs. (12) and (13) are discussed. If both transition rates are equal (Fig. 3), the distributions F_{11} and F_{12} are identical for large thicknesses, as expected. For very low thicknesses F_{11} overwhelms, simply because the interaction time is so small, that hardly any incident particles (state 1) can convert to state 2. With increasing thickness F_{11} decreases and F_{12} increases until finally both are the same. The fact that there is an energy gain for low thicknesses is intrinsic to the diffusion approximation which is strictly valid for large thicknesses only.

If the transition rate $Nv\sigma_{12}$ from the He^+ state (1) to the He^0 state (2) is much larger than the other one, then F_{11} decreases much faster with increasing thickness (Fig. 4) because the conversion to He^0 is much more efficient. For large thickness most of the particles leave the interaction region in this state.

In Fig. 4(a) a new feature is observed at higher energy loss and in Fig. 5 two series of spectra are presented that show how this second maximum evolves when $\sigma_{21} \to 0$. As is most clearly seen in Fig. 5(b), the number of particles scattered into this peak is determined by σ_{12} only. This maximum at 35.9 a.u. originate in those particles that never suffered any neutralization, i.e., the particles surviving in the initial state. This is confirmed by the fact that the integral area below this peak is $\exp(-\sigma_{12}Nx)$, which is just the surviving fraction obtained from the corresponding rate equation. At about the same position there is also a kink in the curve of F_{12}, that can be seen in Fig. 6.

VI. SUMMARY

In Sec. III a recently derived matrix equation for the charge-state distribution was evaluated for two systems: (a) for the case of a proton interacting with an electron gas, using calculated cross sections and (b) for the case of 13 MeV $O^{3+} \rightarrow$ C foil, using experimentally determined cross sections.

Energy-loss spectra for the two-state case were derived in Sec. IV in the diffusion approximation. In the simple case of charge exchange in one direction only, a previously presented formula was rederived.

The expressions obtained for the case of charge exchange in both directions have been evaluated for a number of cases and discussed in Sec. V.

ACKNOWLEDGMENTS

Thanks are due to the Danish Natural Science Research Council (SNF) for generous support, to P. Sigmund for countless helpful discussions, and to J. Wagner and A. Arnau for providing me with the cross section data.

[1] P. Sigmund, in *Interaction of Charged Particles with Solids and Surfaces*, Vol. 271 of *NATO Advanced Study Institute, Series B: Physics*, edited by A. Gras-Martí, H. M. Urbassek, N. R. Aristia, and F. Flores (Plenum Press, New York, 1991), pp. 73–144.

[2] P. Sigmund, Nucl. Instrum. Methods Phys. Res. Sect. B **69**, 113 (1992); this paper also contains an extensive bibliography about charge exchange and energy loss.

[3] A. Närmann and P. Sigmund, Phys. Rev. A **49**, 4709 (1994).

[4] A. Närmann, W. Heiland, R. Monreal, F. Flores, and P. M. Echenique, Phys. Rev. B **44**, 2003 (1991).

[5] A. Meibom, M. Sckerl, A. Närmann, and P. Sigmund, (unpublished).

[6] A. Arnau, M. Peñalba, P. M. Echenique, and F. Flores, Nucl. Instrum. Methods Phys. Res. Sect. B **69**, 102 (1990).

[7] J. Wagner, R. Harder, B. Hertel, J. Maeritz, M. Tempel, H.-G. Toews, and H. Kuiper, Nucl. Instrum. Methods B **73**, 1 (1993).

[8] O. Vollmer, Nucl. Instrum. Methods **121**, 373 (1974).